Shaping a deformable object within a human-robot collaborative framework

Racha Ghaddar, Adrien Koessler, Mourad Benoussaad, Thibaut Raharijaona

Shaping a deformable object within a human-robot collaborative framework

Racha Ghaddar [a], Adrien Koessler [a], Mourad Benoussaad [b], Thibaut Raharijaona [a]

a. Université de Lorraine, Arts et Metiers Institute of Technology, LCFC, F-57070 Metz, France
{racha.ghaddar, adrien.koessler, thibaut.raharijaona} @univ-lorraine.fr
b. LGP-ENIT, Université Technologique Tarbes Occitanie Pyrénées, France
mourad.benoussaad@uttop.fr

Résumé :

La manipulation d'objets souples tels que des câbles, matériaux en feuilles ou tissus est un challenge pour les robots industriels. Dans la littérature, plusieurs méthodes ont été proposées pour asservir la forme d'un objet déformable par des sytsèmes multi-robots. Cependant, dans un tâche de manipulation faisant également collaborer l'humain, le contrôle est plus difficile. En effet, le mouvement humain ne peut être ni négligé, ni prédit. Ce scénario s'applique à des situations industrielles où l'interaction physique humain-robot est nécessaire pour améliorer l'ergonomie et la productivité. Dans cet article, nous étudions une tâche consistant à positionner dans l'espace un unique point matériel d'un objet souple, maintenu à ses deux extrémités par un robot et un humain. Le modèle de chaînette sera utilisé pour modéliser la déformation. Nous proposons une loi de commande proportionnelle évaluée en simulation. Dans ce travail, on propose une commande basée modèle pour le transport coordonné d'un objet déformable par un humain et un robot. Il s'agit d'une première étape pour l'intégration de contributions plus avancées en termes de modélisation par éléments finis et de commande compliante.

Abstract :

Manipulating deformable bodies such as cables, sheets of materials or cloth is a significant challenge for industrial robots. In the literature, many methods are proposed to shape a deformable body using multiple robots. In a human-robot framework however, the shaping process becomes more challenging due to the human dynamics' uncertainties added to the control loop, that can't be neglected or predicted. This scenario is applicable in industrial situations where a human-robot collaborative framework is required to enhance ergonomics and productivity. In this work, we study a task that consists in positioning a single point of an object grasped by a human and a robot at its endpoints. We resort to the theory of catenaries for modeling the object's deformation.For the simulations, we test a proportional control law combined with the interaction Jacobian matrix to validate the whole scheme. This work hence implements a model-based control algorithm that enables collaborative transportation of deformable objects. It represents a first step toward more advanced human-robot deformation control, with future developments potentially integrating real-time finite element model simulation and compliant control.

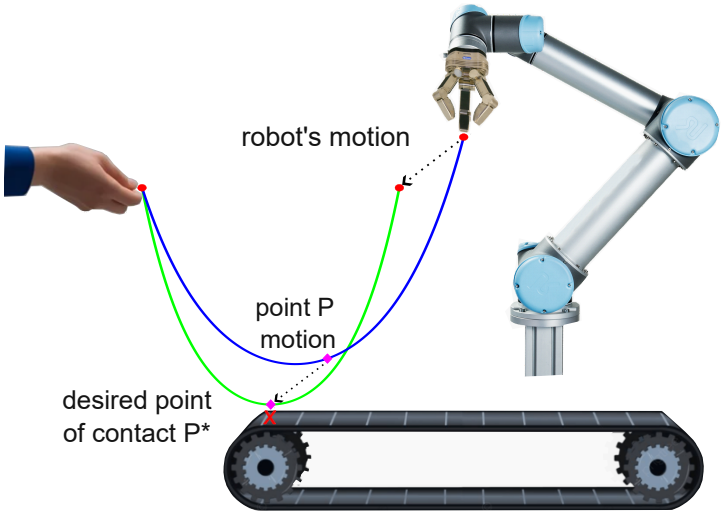

FIGURE 1 – Experimental Setup that shows all the system's elements : Human hand, robot and cable hanged at its endpoints. The goal is to derive point P towards P^* through out controlling the robot's motion responsively.

Keywords : Collaborative Robotics, Human-Robot Interaction, Deformable Objects, Co-manipulation, Catenary Model

1 Introduction

1.1 Conext of the study

Human-robot collaboration is an interdisciplinary field that studies the direct physical interaction between robots and humans to achieve a common goal or task. Hence, developing a human-robot collaborative workplace was the solution to perform faster and more efficient tasks by merging human cognition, awareness, and consciousness with the robot's power generation, capacity, and precision. This field has grown in the past few years resulting in the emergence of Industry 5.0 [1]. Industry 5.0 is the new era of manufacturing that incorporates the human aspect into Industry 4.0, where robots and humans are required to work and interact safely and effectively.

Moreover, some industrial tasks require transporting deformable objects within a specific configuration to avoid material damage or shaping them to reach a given state. This need raises the notion of *deformable object manipulation*, which is an under-actuated problem due to the large number of DOF of the objects. Also the shape and type of the material plays a crucial role in the manipulation process. In such problems, the object deformation should be treated as an objective to be reached. When a task requires a desired shape to be reached, we encounter a problem referred to as *shape control* in the literature [2]. Merging human interaction and deformation of parts, we create a new type of scientific problem. Human dynamics introduce uncertainties to the control loop that cannot be ignored, predicted, or controlled compared to multi-robot, thus the shaping process becomes more challenging.

1.2 Problem Presentation

In this paper, we would like to address the problem of placing a rope-like object (a belt, or a film..) on a desired surface, in such a way that a desired material point on the object will be the first in contact.

The object is grasped by the human and the robot at each end respectively as shown in Figure 1. This application is seen in industry when it is required to layer adhesive sheets or filaments in a desired manner.

The challenges that arise in that context can be divided into three key components of study : perceiving the object shape and the human motion in real-time, modeling the object deformability relative to the actuation points, and controlling the robot motion to get to the desired object configuration considering the human hand dynamics. In this paper we will focus on modeling and control aspects.

This paper proposes a novel catenary-model-based controller that depends on computing the inverse of the *Interaction Jacobian Matrix* (IJM). The objective of this controller is to place a material point of the catenary to a desired position in space by manipulating the position of the robot's end effector reactively to the human hand motion. In our simulations, we will study the trajectory of the point P derived by a inverse IJM proportional controller that outputs the robot's velocity to reach the desired point of contact. We considered two case studies : (i) static human hand, (ii) mobile human hand. In the following sections we will introduce the state of the art, catenary model equations, control law, simulations and discussion.

1.3 Deformable object manipulation

Deformable object manipulation using multi-robot systems is a popular topic in robotics and several surveys were conducted on this topic [6] [7] [8] [9]. The five main elements of a robotic framework for handling deformable objects are typically gripper and robot design, sensing, modeling, planning, and control [3].

Deformable object manipulation has been extended to cases of a human-robot collaborative systems. In such cases the robot and the human are required to transport a deformable body. Several researchers have tackled this problem. For example, De Schepper *et al.* [16] used a model-free hybrid controller based on the wrench and visual data input. On one side, an admittance controller acts as a reactive controller for forces and torques, and on the other side, a vision controller is used as a visual servoing on the robotic arm based on the human's gestures. Sirintuna *et al.* [17], as well, used a model-free adaptive controller, based on measuring the haptic forces transmitted through the deformable object and human gestures detected using motion a motion-capture system. On the contrary, Makris *et al.* [18] tackled the problem of translational and rotational co-manipulation. They proposed a model-based motion planner, where the deformable object is modeled as a spring-damper system. A motion planner algorithm is used to generate the robot's trajectory and monitor the human actions.

1.4 Modeling the deformation

In this paper, we are interested to servo the object deformation, thus deriving a physical model is required. For linear 1D deformable objects like ropes, belts, or tethers, the used model could be simplified into one dimensional space problem. Hence their classification as deformable linear objects (DLO). A detailed review about DLO modeling approaches is conducted by [19]. DLO can be modeled as mass-spring, multi-body, position-based dynamics, finite element, elastic rod, dynamic spline, and data-driven. One of the approaches to model a DLO is using a catenary model in specific cases, where the object is suspended to it's own weight and held from two end-point. We can see this model used in [20] where the authors design and control a *catenary robot* (a cable propelled by two quadrotors). [21] proposes a novel visual servoing approach for catenary-shaped deformable objects, enabling control of the tether's parametric shape by controlling the position of moving mobile robot's, that adjusts the fixation points

of the catenary. [22] used a catenary model and visual data to control the tension in industrial reel, by changing the length of the reel.

The catenary model is a mathematical model. It was encouraged in our case by the fact that it accurately represents the rope shape by a hyperbolic cosine function with exact and analytical solution. This model has a low computational cost since it requires solving a degree one equation.

1.5 Controlling the deformation

Controlling the *object shape* is one of the most interesting and challenging topics in the field on deformable object manipulation. The high deformability of the objects result in different manipulation modeling and control methods, which depends on the object geometry and required application [4]. The shape control problem can be defined as finding the relation between the displacement of the target points on the deformable object with respect to the displacement of the actuated points. This problem can be addressed in different ways, for instance by controlling the objects contour [23], or by controlling the position of a point cloud [24].

One of the most used local models for shape control, is approximating the *interaction Jacobian matrix IJM*. This quantity relates the robot's end-effector velocity with the change in shape of the object [26] [28]. It should be computed in real-time, and updated continuously because it is valid locally [3]. This matrix is generally (pseudo-)inverted to compute a robot motion that produces the desired change in shape. In literature, we can find that the *IJM* is either updated from visual and previous robot displacement data [11] [28] [24], or from the object's model [30] [25] [26] [27]. Other model-based solutions imply solving an optimization problem, where the *IJM* is never explicitely computed [31] [32]. It can be argued, however, that those methods also aim to find which robot motion brings to system closer to its desired configuration, and thus have similar inner workings, eg. the need to perform many forward simulations.

This approach is adopted in shape control algorithms and position control of soft robotics manipulators [31] [32]. However, it has not been used in a human-robot-deformable object interactive framework. This paper presents a innovative model-based approach to control the robot motion in a human-robot collaborative setup. In this paper we consider to simplify the object model into one dimensional, like cables and ropes, to ease the computation of the inverse *IJM* and to verify the use of the *IJM-based controller*. Our goal here is to control the robot's end-effector accordingly to reach a desired object configuration. In the context of our study, this configuration is specified by the desired position of a given material point P belonging to the object.

We claim the following contributions :

- A model that computes in real-time the position of a material point P on the catenary.
- The implementation of an inverse simulation procedure using this catenary-based model.
- A Jacobian-based control law to servo the position of point P.
- The simulation results of the conducted experiments.

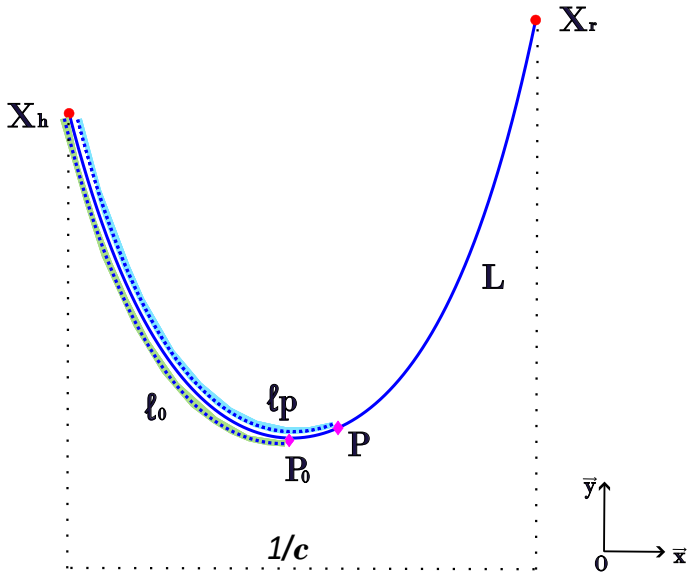

FIGURE 2 – Introducing the catenary parameters : human hand endpoint $\mathbf{x}_h = [x_h, y_h]^T$; robot endpoint $\mathbf{x}_r = [x_r, y_r]^T$; current position of P $\mathbf{x}_p = [x_p, y_p]^T$ at ℓ_p denoted in light blue ; current position of the lowest point on the catenary $P_0(x_0, y_0)$ at ℓ_0 denoted in light green ; catenary geometrical parameter c.

2 Methods

2.1 Modeling the deformation

2.1.1 Catenary Model

The *catenary curve* is the shape taken by a uniform density chain fixed from it's two endpoints and hanging under it's own weight [33]. This model is suitable for cases where the cable has no external contact except for its two end-points. Moreover, our model does not consider the boundary cases where the object is fully stretched horizontally, or aligned vertically (the human and robot endpoints are aligned).

2.1.2 Catenary-based Model Equations

Suppose that H and R are the first and the second endpoints of the catenary held by the human and the robot respectively, and that $O(\vec{x}, \vec{y})$ is the world frame in 2D. Let us denote the coordinates of H in the world frame with the vector $\mathbf{x}_h = [x_h, y_h]^T$ and those of R with $\mathbf{x}_r = [x_r, y_r]^T$. Let P be a material point on the catenary, with world frame coordinates $\mathbf{x}_p = [x_p, y_p]^T$. P is defined by ℓ_p, the arc length from the first endpoint to point P. The total length of the catenary is designated by L so that $0 \leq \ell_p \leq L$. We also introduce $P_0(x_0, y_0)$, the lowest point of the catenary that varies with respect to the catenary shape parameter c. At any point on the catenary the following relation holds :

$$y(x) = y_0 + c\left(\cosh\left(\frac{x - x_0}{c}\right) - 1\right) \tag{1}$$

Thus, the whole shape of the catenary can defined by (c, P_0). In order to estimate the shape of the catenary at each time step we should be able to calculate the values of (c, P_0). We assume that $\mathbf{x}_h$ and

$\mathbf{x}_r$ are perceived in real time, and fed to the deformation model. Using the arc length formula of the catenary we can get the following equation :

$$l_i = \int_{x_h}^{x_0} \sqrt{1 + \left(\frac{dy}{dx}\right)^2}\, dx \tag{2}$$

$$= c \sinh\left(\frac{x_0 - x_h}{c}\right). \tag{3}$$

Applying this equation at both ends yields

$$\frac{L}{c} = \sinh\left(\frac{x_r - x_0}{c}\right) - \sinh\left(\frac{x_h - x_0}{c}\right). \tag{4}$$

We evaluate (1) at H and R, and combine with (4) to compute $(y_r - y_h)^2 - L^2$. It yields :

$$(y_r - y_h)^2 - L^2 = 2c^2 \left(1 - \cosh\left(\frac{x_r - x_h}{c}\right)\right). \tag{5}$$

Having eliminated unknowns x_0, y_0, we can solve (5) for c iteratively using the *Newton-Raphson* method for instance.

Next up, we compute the position of the lowest point $P_0(x_0, y_0)$ on the catenary, as well as its arc length ℓ_0. The main hurdle consists in finding x_0, however this is achieved quite easily by evaluating (1) at H and R and computing the difference :

$$\frac{y_r - y_h}{c} = \cosh\left(\frac{x_r - x_0}{c}\right) - \cosh\left(\frac{x_h - x_0}{c}\right). \tag{6}$$

Using the trigonometric relation for the difference of cosines and isolating x_0 on the right hand side yields :

$$x_0 = \frac{1}{2}\left(x_r + x_h - c \sinh^{-1}\left(\frac{y_r - y_h}{2c \sinh\frac{x_r - x_h}{c}}\right)\right). \tag{7}$$

From them on, plugging x_0 in (1) and (3) yields y_0 and l_0 respectively. Hence, all variables that describe the shape of the catenary are known.

$$\ell_0 = c \sinh\left(\frac{x_0 - x_h}{c}\right) \tag{8}$$

Finally, we find the position of the material point P at a given arc length $s = \ell_p$ using the following equations :

$$x_p = c \cdot \sinh^{-1}\left(\frac{\ell_p - \ell_0}{c}\right) + x_0 \tag{9}$$

$$y_p = c \cdot \sqrt{\left(\frac{\ell_p - \ell_0}{c}\right)^2 + 1} + (y_0 - c) \tag{10}$$

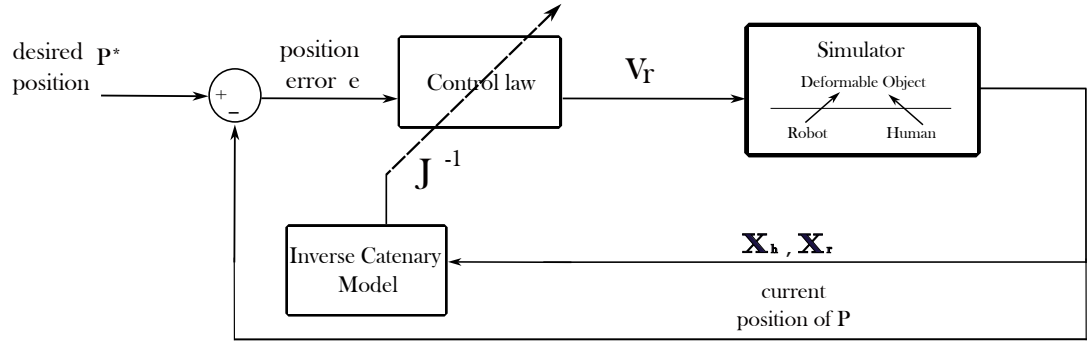

FIGURE 3 – A control scheme that shows the control loop elements : a simulator that simulates the human hand, the robot and the cable, an inverse catenary model that computes the inverse deformation *IJM*, a proportional control law that works on minimizing the position error of point P.

This whole procedure of finding the position $\mathbf{x}_p$ of point P from $\mathbf{x}_r$, assuming known values for $\mathbf{x}_h$ and L, is coined as the forward problem and denoted by the symbol $\mathcal{F}$, so that $\mathbf{x}_p = \mathcal{F}(\mathbf{x}_r)$.

2.2 Controlling the shape deformation

2.2.1 Control problem formulation

In this section, we introduce the control scheme to manipulate a rope-like object using the catenary model introduced in the previous section. The purpose is to control the velocity of the robot's end-effector $\mathbf{v}_r$ to reach the position of point $P(x_p, y_p)$ on the catenary to a desired position $P^*(x_p^*, y_p^*)$. The control problem is a distance minimization problem between the actual position of point P and the desired one P^*, consequently the controller error is defined as follows :

$$\mathbf{e} = \mathbf{x}_p^* - \mathbf{x}_p \tag{11}$$

To put it another way, we will control the robot motion to minimize the error vector $\mathbf{e}$. The full control scheme is represented by Figure 3 that shows the different code blocks needed to perform a closed control loop. The *"MATLAB simulator"* block uses the equations introduced in section 2.1.2 to compute the current position on point P. The *"inverse interaction matrix"* block uses the equation introduced in section 2.2.2 to compute the inverse interaction matrix fed to the *"control block"*. The latter is introduced in section 2.2.3.

2.2.2 *Deformablility interaction matrix* computation

The deformation *IJM* represents the system's gradient that leads to the computation of the direction of the robot motion to minimize the corresponding error [34] [35]. From the local equilibrium position of the robot's end-effector, the system's gradient can be calculated using finite differences. This can be done by applying small displacements $\boldsymbol{\eta}_i$ to robot's position $\mathbf{x}_r$ along each axis, then solving the forward problem to compute the relative change of point P as $\mathbf{x}_p$. Applying the following equation at each time step enables us to estimate the system's deformation *IJM* J :

$$\mathbf{J}[:i] = \frac{\mathcal{F}(\mathbf{x}_r + \boldsymbol{\eta}_i) - \mathcal{F}(\mathbf{x}_r - \boldsymbol{\eta}_i)}{2 \cdot \boldsymbol{\eta}_i} \tag{12}$$

where $\mathbf{J}[:i]$ designates the i-th column of $\mathbf{J}$. In the case where the robot moves in a plane with constant orientation, we have $i \in \{1, 2\}$. $\boldsymbol{\eta}_1 = [\eta, 0]^T$ is the X-axis perturbation and $\boldsymbol{\eta}_2 = [0, \eta]^T$ is the Y-axis perturbation, with $\eta << \mathbf{e}(t = 0)$. This *IJM* will be used in the control law explained in the next section.

2.2.3 Control law synthesis

To servo the position of point P to reach a desired position P^*, we used an exponential decay proportional controller to derive $\mathbf{e}$ to zero. This control law is derived from a first-order dynamic response that can be described as :

$$\dot{\mathbf{e}} + \gamma \mathbf{e} = 0 \tag{13}$$

where γ is the proportional gain. We ensure $\gamma > 0$ for convergence. Let us suppose that the desired position has negligible dynamics. As a result, we can rewrite (13) as :

$$-\dot{\mathbf{x}}_p + \gamma \mathbf{e} = 0. \tag{14}$$

In order to get the controlled actuator $\mathbf{v}_r$ to the previous equation, we need to define a relation between the robot's velocity and the position of point P through the *IJM* as

$$\dot{\mathbf{x}}_p = \mathbf{J}^{-1}\dot{\mathbf{x}}_r = \mathbf{J}^{-1}\mathbf{v}_r. \tag{15}$$

Merging (14) and (15) we get the following velocity control law :

$$\mathbf{v}_r = \mathbf{J}^{-1}\gamma \mathbf{e}. \tag{16}$$

Integrating the computation procedure of the *IJM* and the proportional control law (16), we will now evaluate the whole control loop in simulation experiments.

3 Simulation and Results

3.1 Task description

We consider the task of placing a desired material point P of a rope on a surface at a desired position P^*. The positioning is done collaboratively between a human and a collaborative robotic arm :

- the human is leading the positioning process
- the robot is reactively responding to the human motion to reach the desired position using the control law

The human hand motion is shaky, perturbed, and gradually loses its precision as the distance between the human grasp and the point of interest increases. Hence, using a robot to reach the desired position precisely is encouraged. We conducted two sets of experiments to validate our model-based controller :

- In the first set of experiments, we assumed that the human hand is stationary. The main goal is to verify that we are able to reach the desired position in space using the control law for different values of P^* and ℓ_p.
- In the second experiment, we will show that while the human hand is simultaneously moving, the robot is moving in the direction to minimize the position error, but point P won't be exactly reached due to the constant human hand perturbation.

3.2 Simulation Experiments

The simulation is performed using MATLAB R2023b, in discrete time with a sampling rate $T_s = 2 \cdot 10^{-2}$ s over 300 iterations. This choice is sensible, since the execution time of one control iteration (without plotting or logging) generally stays below this value. We set the initial pose of the human to be $\mathbf{x}_h = [0, 10]^T$ and those of R with $\mathbf{x}_r = [10, 12]^T$ for all of the following experiments. We used the algorithm 1 to simulate our experimental setup with small tweaks for each simulation. The catenary model simulation is done by calling functions *findLowestPoint*, *findLZero*, *findPositionofP* that uses equations (7),(8), (10) respectively, in accordance with the procedure describe at sec. 2.1.1. To implement the control law we called an additional function *inverseJacobian* ; that computes the inverse Jacobian deformation matrix detailed in section 2.2.2.

Algorithm 1 Simulation of the control loop

Input: $\ell_p, \mathbf{x}_p^*$

$\mathbf{x}_{ri} \leftarrow [10, 12]^T$; $\mathbf{x}_h \leftarrow [0, 10]^T$; $L \leftarrow 20; T_s \leftarrow 2e - 2$
$c = catenaryModel(\mathbf{x}_h, \mathbf{x}_{ri}, L)$;
$\mathbf{x}_0 \leftarrow findLowestPoint(\mathbf{x}_h, \mathbf{x}_{ri}, L, c)$;
$\ell_0 = findLZero(\mathbf{x}_h, \mathbf{x}_0, c)$;
$\mathbf{x}_p = findPositionofP(\mathbf{x}_0, \ell_0, \ell_p, c)$;
for $i = 0$ **to** 300 **do**
    $c = catenaryModel(\mathbf{x}_h, \mathbf{x}_r, L)$;
    $\mathbf{x}_0 \leftarrow findLowestPoint(\mathbf{x}_h, \mathbf{x}_r, L, c)$;
    $\ell_0 = findLZero(\mathbf{x}_h, \mathbf{x}_0, c)$;
    $\mathbf{x}_p = findPositionofP(\mathbf{x}_0, \ell_0, \ell_p, c)$;
    $\mathbf{J}^{-1} = inverseJacobian(\mathbf{x}_h, \mathbf{x}_r, L, \ell_p)$;
    $\mathbf{e} = \mathbf{x}_p^* - \mathbf{x}_p$;
    $\mathbf{v}_r = \gamma * \mathbf{J}^{-1} * \mathbf{e}$;
    $\mathbf{x}_r = \mathbf{x}_r + T_s \cdot \mathbf{v}_r$;
end for

3.2.1 Reaching various configurations

For the first set of the experiments we focused on studying the controller capability of reaching a desired position. We conducted several simulation to prove the convergence of P_i towards P^* by changing P^* and ℓ_p. Fig. 4 shows the simulation results. The initial catenary is drawn in blue while the red catenaries shows the updated catenary shape over each time step. The pink diamond marks the position of P^* and the blue ones show the trajectory of point P at each time step until it reaches the desired position P^*. As seen in the figure and confirmed by quantitative validation, the position of point P converges exponentially towards the desired value for all four tested configurations. This result is sensible given the proportional nature of the control law and the absence of any perturbation, and validates the soundness of our approach.

3.2.2 Implementing the human motion

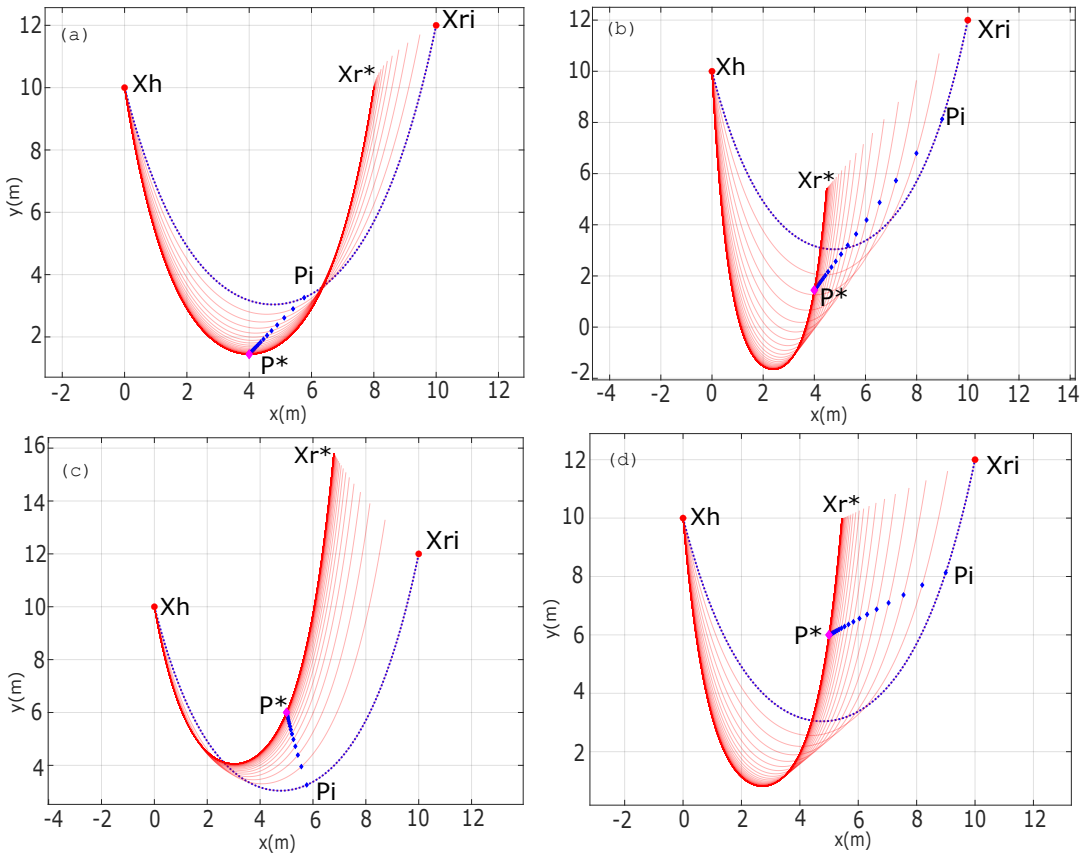

FIGURE 4 – Baseline simulations without human motion that shows the convergence of P from its initial position towards P^* the desired position. We conducted several tests by changing the values of P^* and ℓ_p to insure convergence toward different desired positions. (a) $\mathbf{x}_p^* = [4, 1.44497]$, ℓ_p = 10; (b) $\mathbf{x}_p^* = [4, 1.44497]$, ℓ_p = 16; (c) $\mathbf{x}_p^* = [5, 6]$, ℓ_p = 10; (d) $\mathbf{x}_p^* = [5, 6]$, ℓ_p = 16.

In this second step, we want to assess the influence of the human motion on the controller's outcomes. To this end, a human motion was applied as a perturbation at the first catenary grasp point.

$$x_h(t) = x_h(t=0) + a_h\left(\cos(2\pi f_h t) - 1\right) \tag{17}$$

$$y_h(t) = y_h(t=0) + a_h \sin(2\pi f_h t) \tag{18}$$

where a_h is the amplitude of the human motion (in m) and f_h its frequency in Hz. This circular motion is not meant to simulate a purposeful human motion, but rather its shakiness when trying to stand still. We set $a_h = L/100$ =0.2 m for testing purposes. Our aim is to assess the trade-off between the proportional gain and the frequency of the perturbation. To this end, we calculated the RMS error, that is to say the RMS value of the distance between the desired and current position of point P. We simulated the setup for different values of f_h and control gains γ. Table 1 shows the obtained results.

This table shows that for small gains $\gamma = 2 \times 10^{-3}$ and $\gamma = 2 \times 10^{-2}$ the controller remains inefficient compared to the amplitude of the human hand perturbation a_h = 0.2 m. As we can see that the RMS error remains very large in all trials meaning that the controller almost has no influence. As we increase the gain value to $\gamma = 2 \times 10^{-1}$, the controller efficiently counters the human hand motion at lower

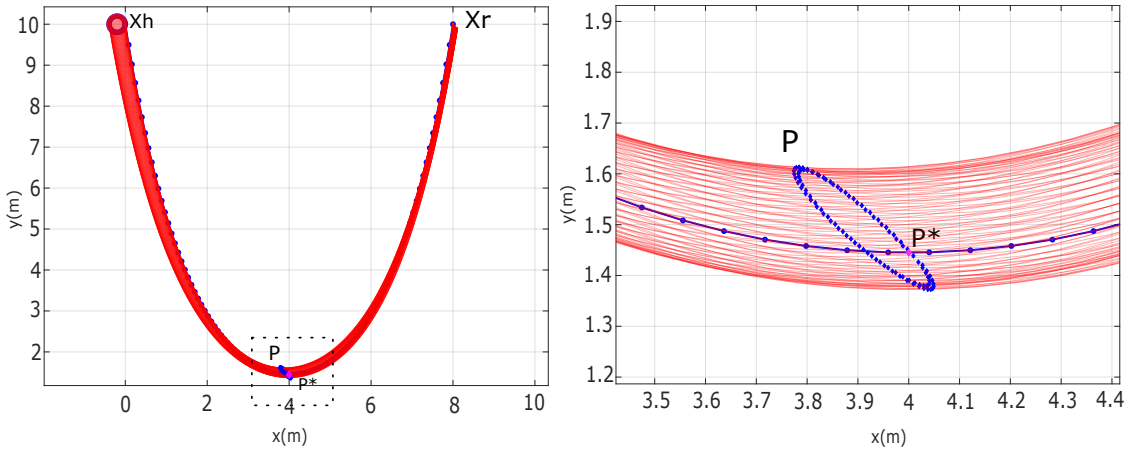

FIGURE 5 – Simulation involving human motion perturbation on the first rope grasping point, and the corresponding robot's end-effector motion at the second grasping point to ensure placing point P at it's desired position P^*. (a) $\mathbf{x}_p^* = [4, 1.44497]$, ℓ_p= 10; (b) image zoom towards point P trajectory.

γ (s^{-1}) \ f_h(Hz)	0.5	1	2	5	10
2×10^{-3}	0.16126	0.15205	0.1518	0.15162	0.15156
2×10^{-2}	0.10977	0.12802	0.13251	0.13323	0.13311
2×10^{-1}	0.01979	0.03838	0.06964	0.11637	0.13486
2×10^{0}	0.00298	0.00582	0.01149	0.03008	∞

TABLE 1 – Values for RMS position error (in m) with different gains and human motion frequencies.

frequencies (f_h = 0.5, 1 Hz), but has limited bandwidth and ends up being incapable of servoing the position under higher frequency perturbation (f_h = 2, 5, 10 Hz). Then as we stiffen the control gain up to $\gamma = 2 \times 10^0$, the RMS error reached it's optimum values at lower frequencies, thus the controller performs the best. But it induces instability at the higher end of the perturbation frequency range.

As a general behavior trend, we can see that for a certain gain value, the controller performance degrades as we increase the human hand frequency. We can conclude that the proportional controller can stand at lower frequencies, but it is not adequate at higher ones. To that end, we must use a more responsive controller to handle different human dynamic demands and fast human inputs.

4 Conclusion and Discussion

In this article, we have proposed a catenary model-based controller to control the robot's velocity responsively to the human motion, for the purpose of placing a material point on the catenary at a desired surface. With that aim, we proposed a catenary-based model that computes the position of point P in real-time. Using this model we implemented an inverse simulation that computes the deformation *interaction Jacobian matrix* inputted to a proportional control law. The verification of the contributed method was tested on MATLAB in simulation. For further steps, we would like to control the position of the robot's end effector such that point P is the lowest point on the catenary to ensure that P is the first point in contact on the desired surface position. As a consequence controlling ℓ_p is required. Also for future work, we wish to test our control law on a real human-robot-deformable object system. For that purpose,

we will use a vision system to track the position of the human hand in real time, and to track the position of point P as a ground truth to our method. Also, we would like to improve our controller to a more compliant and responsive one that handles higher human frequency inputs. Also future work will focus on incorporating the dynamics of the object model by extending the current analytical catenary representation to a finite element model. This will allow us to study the evolution of system performance as a function of disturbance frequency and to systematically evaluate the robustness of the control system.

Références

[1] Dhanda, M., Rogers, B. A., Hall, S., Dekoninck, E., Dhokia, V. (2025). Reviewing human-robot collaboration in manufacturing : Opportunities and challenges in the context of industry 5.0. Robotics and Computer-Integrated Manufacturing, 93, 102937.

[2] Das, J., Sarkar, N. (2011). Autonomous shape control of a deformable object by multiple manipulators. Journal of Intelligent Robotic Systems, 62, 3-27.

[3] Zhu, J., Cherubini, A., Dune, C., Navarro-Alarcon, D., Alambeigi, F., Berenson, D. Gienger, M. (2022). Challenges and outlook in robotic manipulation of deformable objects. IEEE Robotics Automation Magazine, 29(3), 67-77.

[4] Sanchez, J., Corrales, J. A., Bouzgarrou, B. C., Mezouar, Y. (2018). Robotic manipulation and sensing of deformable objects in domestic and industrial applications : a survey. The International Journal of Robotics Research, 37(7), 688-716.

[5] Ajoudani, A., Zanchettin, A. M., Ivaldi, S., Albu-Schäffer, A., Kosuge, K., Khatib, O. (2018). Progress and prospects of the human–robot collaboration. Autonomous robots, 42, 957-975.

[6] Jiménez, P. (2012). Survey on model-based manipulation planning of deformable objects. Robotics and computer-integrated manufacturing, 28(2), 154-163.

[7] Herguedas, R., López-Nicolás, G., Aragüés, R., Sagüés, C. (2019, September). Survey on multi-robot manipulation of deformable objects. In 2019 24th IEEE International Conference on Emerging Technologies and Factory Automation (ETFA) (pp. 977-984). IEEE.

[8] Nadon, F., Valencia, A. J., Payeur, P. (2018). Multi-modal sensing and robotic manipulation of non-rigid objects : A survey. Robotics, 7(4), 74.

[9] Arriola-Rios, V. E., Guler, P., Ficuciello, F., Kragic, D., Siciliano, B., Wyatt, J. L. (2020). Modeling of deformable objects for robotic manipulation : A tutorial and review. Frontiers in Robotics and AI, 7, 82.

[10] Yoshida, E., Ayusawa, K., Ramirez-Alpizar, I. G., Harada, K., Duriez, C., Kheddar, A. (2015, June). Simulation-based optimal motion planning for deformable object. In 2015 IEEE international workshop on advanced robotics and its social impacts (ARSO) (pp. 1-6). IEEE.

[11] Zhu, J., Navarro-Alarcon, D., Passama, R., Cherubini, A. (2021). Vision-based manipulation of deformable and rigid objects using subspace projections of 2D contours. Robotics and Autonomous Systems, 142, 103798.

[12] Mitsioni, I., Karayiannidis, Y., Stork, J. A., Kragic, D. (2019, October). Data-driven model predictive control for the contact-rich task of food cutting. In 2019 IEEE-RAS 19th International Conference on Humanoid Robots (Humanoids) (pp. 244-250). IEEE.

[13] Jia, B., Hu, Z., Pan, J., Manocha, D. (2018, May). Manipulating highly deformable materials using a visual feedback dictionary. In 2018 IEEE International Conference on Robotics and Automation (ICRA) (pp. 239-246). IEEE.

[14] Cherubini, A., Ortenzi, V., Cosgun, A., Lee, R., Corke, P. (2020). Model-free vision-based shaping of deformable plastic materials. The International Journal of Robotics Research, 39(14), 1739-1759.

[15] Yin, H., Varava, A., Kragic, D. (2021). Modeling, learning, perception, and control methods for deformable object manipulation. Science Robotics, 6(54), eabd8803.

[16] De Schepper, D., Schouterden, G., Kellens, K., Demeester, E. (2023). Human-robot mobile co-manipulation of flexible objects by fusing wrench and skeleton tracking data. International Journal of Computer Integrated Manufacturing, 36(1), 30-50.

[17] Sirintuna, D., Giammarino, A., Ajoudani, A. (2022, October). Human-robot collaborative carrying of objects with unknown deformation characteristics. In 2022 IEEE/RSJ International Conference on Intelligent Robots and Systems (IROS) (pp. 10681-10687). IEEE.

[18] Makris, S., Kampourakis, E., Andronas, D. (2022). On deformable object handling : Model-based motion planning for human-robot co-manipulation. CIRP Annals, 71(1), 29-32.

[19] Almaghout, K., Cherubini, A., Klimchik, A. (2024). Robotic co-manipulation of deformable linear objects for large deformation tasks. Robotics and Autonomous Systems, 175, 104652.

[20] D'antonio, D. S., Cardona, G. A., Saldana, D. (2021). The catenary robot : Design and control of a cable propelled by two quadrotors. IEEE Robotics and Automation Letters, 6(2), 3857-3863.

[21] Laranjeira, M., Dune, C., Hugel, V. (2017, May). Catenary-based visual servoing for tethered robots. In 2017 IEEE International Conference on Robotics and Automation (ICRA) (pp. 732-738). IEEE.

[22] Filella, N. R., Koessler, A., Bouzgarrou, B. C., Ramon, J. A. C. (2022, October). 3D visual-based tension control in strip-like deformable objects using a catenary model. In 2022 IEEE/RSJ International Conference on Intelligent Robots and Systems (IROS) (pp. 3210-3217). IEEE.

[23] Cuiral-Zueco, I., Karayiannidis, Y., López-Nicolás, G. (2023). Contour based object-compliant shape control. IEEE Robotics and Automation Letters, 8(8), 5164-5171.

[24] Saghour, C., Navarro-Alarcón, D., Fraisse, P., Cherubini, A. (2024). Dual-arm shaping of soft objects in 3D based on visual servoing and online FEM simulations. The International Journal of Robotics Research, 02783649241301076.

[25] Koessler, A., Filella, N. R., Bouzgarrou, B. C., Lequièvre, L., Ramon, J. A. C. (2021, May). An efficient approach to closed-loop shape control of deformable objects using finite element models. In 2021 IEEE International conference on robotics and automation (ICRA) (pp. 1637-1643). IEEE.

[26] Shetab-Bushehri, M., Aranda, M., Mezouar, Y., Özgür, E. (2023). Lattice-based shape tracking and servoing of elastic objects. IEEE Transactions on Robotics, 40, 364-381.

[27] Artinian, A., Amar, F. B., Perdereau, V. (2024). Closed-loop shape control of deformable linear objects based on Cosserat model. IEEE Robotics and Automation Letters.

[28] Navarro-Alarcon, D., Yip, H. M., Wang, Z., Liu, Y. H., Zhong, F., Zhang, T., Li, P. (2016). Automatic 3-d manipulation of soft objects by robotic arms with an adaptive deformation model. IEEE Transactions on Robotics, 32(2), 429-441.

[29] Saghour, C., Navarro-Alarcón, D., Fraisse, P., Cherubini, A. (2024). Dual-arm shaping of soft objects in 3D based on visual servoing and online FEM simulations. The International Journal of Robotics Research, 02783649241301076.

[30] Courtecuisse, H., Allard, J., Kerfriden, P., Bordas, S. P., Cotin, S., Duriez, C. (2014). Real-time simulation of contact and cutting of heterogeneous soft-tissues. Medical image analysis, 18(2), 394-410.

[31] Bieze, T. M., Largilliere, F., Kruszewski, A., Zhang, Z., Merzouki, R., Duriez, C. (2018). Finite element method-based kinematics and closed-loop control of soft, continuum manipulators. Soft robotics, 5(3), 348-364.

[32] Coevoet, E., Escande, A., Duriez, C. (2019, April). Soft robots locomotion and manipulation control using FEM simulation and quadratic programming. In 2019 2nd IEEE International Conference on Soft Robotics (RoboSoft) (pp. 739-745). IEEE.

[33] Yates, R. C. (1974). Curves and Their Properties.

[34] Adagolodjo, Y., Goffin, L., De Mathelin, M., Courtecuisse, H. (2019). Robotic insertion of flexible needle in deformable structures using inverse finite-element simulation. IEEE Transactions on Robotics, 35(3), 697-708.

[35] Baksic, P., Courtecuisse, H., Duriez, C., Bayle, B. (2020, May). Robotic needle insertion in moving soft tissues using constraint-based inverse Finite Element simulation. In 2020 IEEE International Conference on Robotics and Automation (ICRA) (pp. 2407-2413). IEEE.